



# MultiCardioNet: Interoperability between ECG and PPG biometrics

Ruggero Donida Labati <sup>a,\*</sup>, Vincenzo Piuri <sup>a</sup>, Francesco Rundo <sup>b</sup>, Fabio Scotti <sup>a</sup>

<sup>a</sup> Department of Computer Science, Università degli Studi di Milano, via Celoria, 18, I-20133 Milano (MI), Italy

<sup>b</sup> STMicroelectronics, ADG, Central R&D, 95121 Catania (CT), Italy

## ARTICLE INFO

Editor: Maria De Marsico

### Keywords:

Biometrics  
ECG  
PPG  
Interoperability  
Siamese networks

## ABSTRACT

Compared to other well-known biometric technologies based on physiological traits (e.g., fingerprint, iris, and face), heart biometrics are more robust to presentation attacks and are particularly suitable for continuous/periodic recognition. Most studies on heart biometrics concern electrocardiogram (ECG) and photoplethysmogram (PPG). While the reported results are encouraging, to the best of our knowledge, no studies have been conducted on the interoperability between ECG and PPG biometrics. We present a novel method that is capable of performing single-domain and multiple-domain identity verifications for ECG and PPG signals, providing interoperability between the heterogeneous cardiac signals. Our method does not require the computation of any reference/fiducial point and uses a compact representation of the given signals. We propose MultiCardioNet, a novel Siamese neural network trained by using an ad hoc learning algorithm. MultiCardioNet computes a similarity score between two spectrogram-based representations of cardiac signals. Our learning algorithm iteratively computes a balanced subset of genuine and impostor pairs during the training epochs. We performed experiments on a dataset containing 1,008 pairs of ECG and PPG samples, obtaining accuracy comparable to that of the state-of-the-art methods for single-domain scenarios and demonstrating only a relatively small performance decrease in the multiple-domain scenario.

## 1. Introduction

Physiological signals pertain to the class of hidden biometrics, which cannot be seen by the naked eye. Physiological signals are usually collected by adopting dedicated sensors placed on the surface of the human body. Most studies in the literature conducted on biometric systems based on physiological signals concern brain biometrics [1,2] and heart biometrics [3].

The wide diffusion of wearable and portable sensors makes heart biometrics particularly attractive physiological traits for a wide range of biometric recognition applications. Heart biometrics include different cardiac signals, such as ECG, PPG, seismocardiogram (SCG), and phonocardiogram (PCG) signals.

A relevant advantage of heart biometrics over other biometric traits (e.g., fingerprints, irises, and faces) is their greater robustness to presentation attacks [4,5] since cardiac signals can be acquired only from living individuals by using specific devices. Furthermore, heart biometrics are particularly suitable for continuous/periodical recognition since the samples can be acquired over long periods in a continuous manner, without requiring any specific action from the users [6]. Additionally, cardiac signals can be used to perform biometric recognition

in already deployed systems for health care or wellness applications by sharing the same acquisition hardware.

The most widely used technologies for the analysis of cardiac signals are based on ECG or PPG acquisition devices. An electrocardiograph is a signal recorded by the electric potential changes occurring between electrodes placed on different body parts. ECGs are frequently acquired from multiple leads by using medical devices [7]. In contrast, a PPG is a noninvasive technique for measuring blood perfusion through tissues via the emission of light radiation [8]. The acquisition devices used are typically less expensive than ECG-based devices and are frequently adopted for monitoring sport activities.

Recently developed wearable devices can integrate technologies for acquiring and processing both ECG and PPG signals. As an example, recent smartwatches have integrated ECG and PPG acquisition sensors. In most cases, however, these devices can only acquire ECG signals for a limited period by requiring user cooperation. In contrast, most PPG sensors integrated into smartwatches and wristbands can acquire signals continuously over time without requiring any user cooperation.

In the literature, different studies on ECG [9] and PPG [10] biometrics have been conducted. The studies on ECG biometrics achieved better accuracy on datasets composed of larger sets of individuals than

\* Corresponding author.

E-mail addresses: [ruggero.donida@unimi.it](mailto:ruggero.donida@unimi.it) (Ruggero Donida Labati), [vincenzo.piuri@unimi.it](mailto:vincenzo.piuri@unimi.it) (V. Piuri), [francesco.rundo@st.com](mailto:francesco.rundo@st.com) (F. Rundo), [fabio.scotti@unimi.it](mailto:fabio.scotti@unimi.it) (F. Scotti).

<https://doi.org/10.1016/j.patrec.2023.09.009>

Received 18 April 2023; Received in revised form 24 August 2023; Accepted 22 September 2023

Available online 25 September 2023

0167-8655/© 2023 The Authors. Published by Elsevier B.V. This is an open access article under the CC BY license (<http://creativecommons.org/licenses/by/4.0/>).

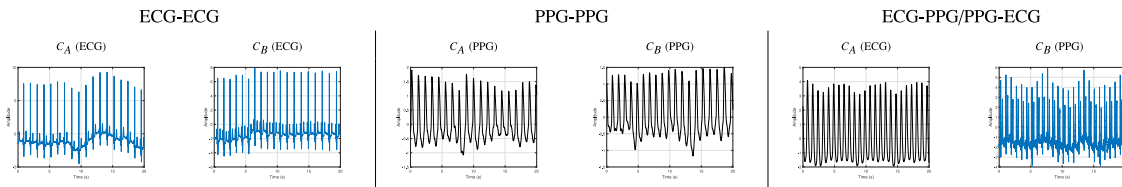


Fig. 1. Examples of single-domain and multiple-domain cardiac signals processable by the proposed identity verification method: (i) ECG-ECG signals; (ii) PPG-PPG signals; (iii) ECG-PPG/PPG-ECG signals. For each configuration, the cardiac signals  $C_A$  and  $C_B$  were collected from the same individual.

that of studies on PPG biometrics [3]. Furthermore, the stability of ECG biometrics has been analyzed for longer acquisition periods [11] and for acquisitions performed across greater time differences [12] relative to PPG biometrics. ECG-based biometric technologies can therefore be considered more mature than PPG-based biometric technologies. Studies have proven the feasibility of performing biometric recognition on PPG signals acquired in more challenging conditions than those considered for ECG signals. For example, systems can perform biometric recognition to analyze the PPG signals acquired during sport activities [13].

In our proposal, the biometric system is capable of processing ECG and PPG biometrics by guaranteeing their interoperability, therefore exploiting the advantages of both types of cardiac signals. As an example, a system integrated into a smartwatch can periodically perform more trusted identity recognitions by using ECG signals and perform continuous/periodical biometric recognition by using PPG signals. Furthermore, the PPG signals acquired with economic wearable devices can be used to access systems in which the users have been enrolled by using ECG signals acquired using medical devices. To the best of our knowledge, no studies in the literature have considered the interoperability between ECG and PPG biometrics.

In this paper, we present a novel method designed for single-domain and multiple-domain identity verification based on cardiac signals. Our method can compare the following pairs of signals: (i) ECG-ECG, (ii) PPG-PPG, and (iii) ECG-PPG/PPG-ECG signals. The developed biometric recognition method is based on a novel deep neural network (DNN), called MultiCardioNet, which consists of a Siamese convolutional neural network (CNN) [14] trained by using an ad hoc learning algorithm. Fig. 1 shows examples of the considered pairs of signals.

Considering single-domain modalities, an advantage of our method over many techniques in the literature based on heart biometrics is that our method does not need to compute any reference/fiducial points, thus being robust to the possible failures of point detection algorithms. For this purpose, we use a two-dimensional representation of the cardiac signals, which is less sensitive to time shifts than the methods based on one-dimensional signals [15]. To the best of our knowledge, this is the first attempt to apply DNNs based on two-dimensional representations of PPG biometrics. Furthermore, our method is based on a compact representation of the given cardiac signals, which can simplify its use in edge devices, such as mobile phones and wearable technologies. In distributed systems, performing most of the computations on edge devices can reduce the computational load of the server and the inherent privacy risks by not sending biometric samples over the network [16].

Our method computes biometric templates as the embeddings obtained by the proposed MultiCardioNet. The identity comparison is computationally efficient since the matching score is calculated as the Euclidean distance between templates.

Frequently, the limited number of samples present in public cardiac signal datasets can represent an obstacle when designing accurate DNNs. To overcome this limitation, we also present an ad hoc training algorithm for Siamese neural networks.

The proposed novelty is threefold.

1. We present the first study on the interoperability between ECG and PPG biometrics based on Siamese CNNs.

2. We propose a novel identity verification approach using CNNs for processing the two-dimensional representations of PPG signals.

3. We present an ad hoc algorithm for training identity verification systems based on Siamese CNNs, which is suitable for unbalanced datasets with limited numbers of samples.

We validated the proposed method by using the publicly available CapnoBase PRRB dataset [17], including ECG and PPG pairs of signals collected from 42 individuals. For single-domain comparisons among ECG and PPG samples, we obtained accuracy comparable to that of the state-of-the-art techniques and only a relatively small performance decrease in the considered multiple-domain scenario (ECG-PPG/PPG-ECG). Furthermore, we experimentally evaluated the performance of the proposed training algorithm, obtaining the best strategy for single-domain and multiple-domain identity comparisons.

The remainder of the paper is structured as follows. Section 2 analyzes the related works on heart biometrics and on Siamese neural networks for biometric recognition. Section 3 presents our proposed method. Section 4 describes the experimental protocol and obtained results. Section 5 concludes the work.

## 2. State-of-the-art methods

### 2.1. Heart biometrics

Most of the studies in the literature conducted on heart biometrics are based on ECG signals [3]. Furthermore, these studies consider signals acquired over long time spans and use on-the-body and off-the-body sensors [9]. Recent works on PPG biometrics proved that this type of signal presents sufficient biometric discriminability for a wide range of applications [10]. As an example, recent studies proved the feasibility of recognizing individuals from PPG signals acquired during sport activities [18].

Recognition methods designed for ECG signals can be classified into fiducial methods and nonfiducial methods [19]. Fiducial points are six characteristic points (P, Q, R, S, T, and U) that are present in healthy ECG signals. The first class of methods frequently extracts signal characteristics with respect to the positions of the fiducial points and applies a matching method that compares the extracted features [20]. Some fiducial methods only extract R points to temporarily align portions of ECG signals by considering the signal portions as biometric templates [21]. The main problem with fiducial methods is that they are not robust to possible failures of the algorithms used to detect the fiducial points [22]. Nonfiducial methods directly extract features from ECG signals but usually need more complicated matchers [22]. The methods in the literature can consider complete heartbeats [23] or only the QRS complex, which is the most stable portion of the signal to emotional and physical variations [11].

Recognition methods designed for ECG signals can be based on algorithmic approaches [6], machine learning techniques for the analysis of handcrafted features [24], or DNNs [25]. Most of the best-performing methods in the literature are based on CNNs [26] or deep belief networks [27] designed to process one-dimensional signals. In contrast, to reduce the problems caused by temporal misalignments between ECG signals, some studies have computed two-dimensional representations

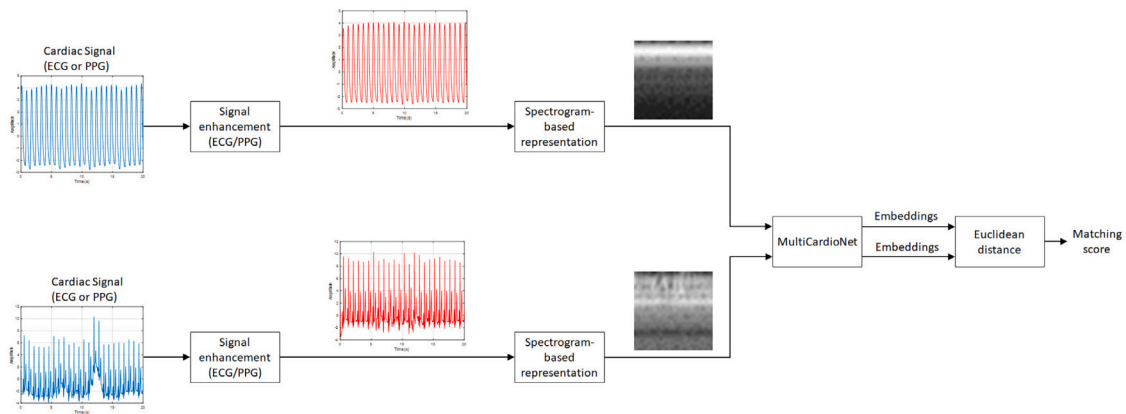


Fig. 2. Schema of the proposed method.

of ECG signals, such as spectrograms [28], scalograms [29], or modified versions of the continuous wavelet transform [30].

Most of the studies in the literature on PPG-based biometric recognition use a strategy similar to that of fiducial methods by selecting the systolic peaks to align PPG signals [31]. Only a limited number of studies are based on nonfiducial methods [32]. Biometric systems based on PPG signals can use algorithmic approaches [33], machine learning techniques for the analysis of handcrafted features [34], or DNNs [35]. Most of the best-performing methods are based on CNNs [36].

To the best of our knowledge, most of the methods in the literature are based on the analysis of one-dimensional signals; only one study on PPG biometrics computes two-dimensional representations of cardiac signals, which is based on support vector machines [15]. In contrast, this paper proposes the use of two-dimensional CNNs for PPG biometrics.

Although studies have been conducted on fusion strategies based on ECG and PPG biometrics [37], to the best of our knowledge, no studies have considered the interoperability between ECG and PPG signals for biometric applications.

## 2.2. Siamese neural networks for biometric recognition

Siamese neural networks have been successfully adopted for single-domain as well as cross-domain biometrics. Single-domain applications aim at performing identity verifications based on samples of the same biometric trait acquired in comparable conditions using similar sensors. Siamese neural networks can be successfully applied in biometric recognition systems based on different traits, for example, based on face [38] or behavioral biometrics [39]. Studies have also been conducted on Siamese neural networks for ECG biometrics [40,41], reporting encouraging accuracy. On datasets containing ECGs collected from 90 individuals, the method presented in [40] achieved 86.47% classification accuracy, while the method described in [41] attained 96.31% classification accuracy.

Cross-domain biometric applications of Siamese neural networks aim at comparing samples presenting relevant differences due to acquisition sensors or acquisition conditions. As an example, Siamese neural networks can be used to compare fingerprint images acquired using touchless and touch-based sensors [42] or heterogeneous touch-based sensors [39]. Another example consists of comparing biometric data collected using different virtual reality devices [43].

Inspired by the encouraging results reported in the literature, we designed a Siamese CNN for single-domain and cross-domain cardiac biometrics.

## 3. The proposed method

To the best of our knowledge, the proposed method is the first technique in the literature that is able to perform biometric recognition based on heterogeneous cardiac signals. Specifically, our method performs identity verifications between two samples (pairs of ECG-ECG, PPG-PPG, ECG-PPG, and PPG-ECG signals). The method is based on the proposed deep neural network called MultiCardioNet, which consists of a novel Siamese CNN trained using an ad hoc algorithm. The biometric recognition method can be divided into the following steps: (i) signal enhancement, (ii) computation of a spectrogram-based representation of the given cardiac signals, and (iii) identity comparison based on the proposed MultiCardioNet. Fig. 2 shows the schema of the proposed identity verification method.

Apart from the preprocessing task, which requires noise reduction strategies specific to each kind of cardiac signal, all the other computational tasks of our method are identical for both ECG and PPG signals.

The computation of a spectrogram-based representation of cardiac signals aims at increasing the robustness of the identity verification process to time shifts between the cardiac signals. To the best of our knowledge, our method is the first approach in the literature that uses DNNs based on two-dimensional representations of PPG signals.

We design the two-dimensional Siamese CNN (MultiCardioNet) to compare the spectrogram-based representations of cardiac signals, with the aim of achieving strong accuracy while using limited computational resources. To train MultiCardioNet, we also design an ad hoc training algorithm for Siamese neural networks, which is inspired by techniques presented in the literature for selecting the triplets used to train facial recognition systems based on the triplet loss [44]. Different from algorithms designed for the triplet loss, we select pairs of samples. Another difference is the fact that facial recognition systems are usually trained using datasets containing billions of images, while cardiac sample datasets are typically composed of much smaller numbers of samples. Therefore, we specifically design and tune our training algorithm for unbalanced datasets composed of relatively small numbers of samples.

Feature extraction is performed by CNNs sharing the same architecture and weights, and the matching process is based on a symmetric function (the Euclidean distance between the templates). Therefore, we consider the comparisons among ECG-PPG and PPG-ECG samples as a single application scenario (ECG-PPG/PPG-ECG).

### 3.1. Signal enhancement

To enhance ECG and PPG signals, we apply filtering techniques that are widely used in the literature, which were specifically designed for every considered type of cardiac signal.

For ECG signals, we first reduce the noise introduced by the power transmission line by applying a notch IIR filter consisting of a Butterworth band-stop filter. Specifically, we use fourth-order Butterworth notch filters with a 3-dB stopband to reduce 50-Hz power line noise interference. We then normalize the signal's baseline by using a third-order high-pass Butterworth filter with a cutoff frequency of  $f_b$ .

For PPG signals, we apply a second-order high-pass Butterworth filter with a cutoff frequency of  $f_h$  and a sixth-order low-pass Butterworth filter with a cutoff frequency of  $f_l$ .

The amplitude response of a low-pass Butterworth filter approximates the function  $|H(e^{j\omega})| = 1 / \sqrt{1 + (\omega/\omega_c)^{2N}}$ , where  $\omega_c = 2\pi f_c/f_s$ ,  $f_c$  is the cutoff frequency,  $f_s$  is the sampling frequency, and  $N$  is the filter order.

### 3.2. Spectrogram-based representation of cardiac signals

The main goal of this step is to perform a discriminative two-dimensional transformation on the input signal, and this process is similar for both PPG and PPG samples. Furthermore, by using a spectrogram-based representation, we increase the robustness of the biometric recognition approach to time misalignments between cardiac signals with respect to their one-dimensional representations; thus, we do not need to compute reference/fiducial points to align ECG and PPG signals.

We first compute a spectrogram-based representation  $I$  starting from the input cardiac signal  $x$  by using the approach described in [15]. We consider the spectrogram as an intensity plot of the squared short-time Fourier transform (STFT) magnitude. The STFT is a sequence of FFTs for windowed data segments, where the windows are usually allowed to overlap in time. A simple notation for defining the STFT of the input signal  $\hat{X}$  is as follows:

$$\hat{X} = \bar{F}X, \quad (1)$$

$$X = (1/m)F\hat{X}, \quad (2)$$

where  $\bar{F}$  is the complex conjugate of  $F$  and  $F$  is the Fourier matrix. We choose sliding windows of size  $m$  and overlap  $o_m$ .

Although many works compute spectrogram images as logarithmic representations of the power spectral density, to obtain a more discriminative representation of the signals, we first compute a pseudo image  $I_p$  composed of three channels ( $A, B, C$ ).

For each row  $r$  of  $\hat{X}$ , we define  $A(i)$  as:

$$A(r) = f/f_{max}, \quad (3)$$

where  $f$  are frequencies and  $f_{max}$  is the maximum of  $f$ .

The matrix  $B$  is obtained as follows:

$$B = L/L_{max}, \quad (4)$$

$$L = \log_{10}(1 + 10 \times (D'_s)), \quad (5)$$

$$D' = (D - D_{min}) / (D_{max} - D_{min}), \quad (6)$$

where  $D$  is the power spectral density or the power spectrum of each segment,  $D_{min}$  is the minimum value of  $D$ ,  $D_{max}$  is the maximum value of  $D$ , and  $L_{max}$  is the maximum value of  $L$ .

The matrix  $C$  is obtained as follows:

$$C = [(D - D_{min}) / (D_{max} - D_{min})]^{0.2}. \quad (7)$$

We compute  $I$  by converting  $I_p$  from the HSV color space to the RGB color space and selecting the red channel.

Since we observe that most of the distinctive information is present in the upper part of  $I$ , we compute  $I'$  by cropping  $I$  to a height of  $y_c$  pixels. We finally obtain  $S$  by resizing  $I'$  to the image size accepted by MultiCardioNet.

Fig. 3 shows examples of spectrogram-based representations  $S$  obtained from ECG and PPG signals. (a) and (c) are acquired from the same individual at the same time instant. (b) and (d) are acquired from

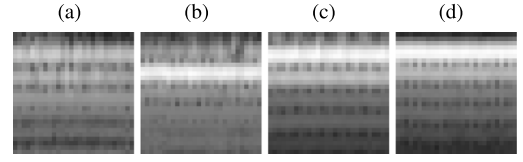


Fig. 3. Examples of the spectrogram-based representations of cardiac signals. (a) and (c) are acquired from the same individual at the same time instant. (b) and (d) are acquired from a different individual at the same time instant. (a) and (c) are computed from ECG signals, while (c) and (d) are computed from PPG signals. The spectrogram-based representations of ECG and PPG signals derived from the same individual present visual differences in their patterns and should therefore be matched by using specifically designed techniques. The spectrograms obtained from cardiac signals present relevant differences that can also be recognized by human operators.

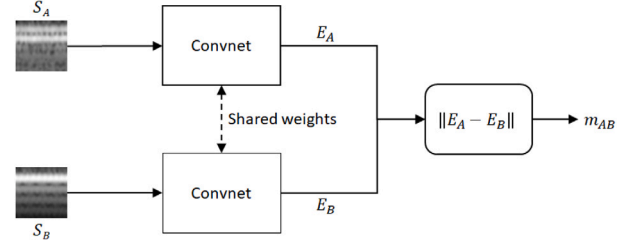


Fig. 4. Schema of the proposed MultiCardioNet deep neural network.

a different individual at the same time instant. (a) and (c) are computed from ECG signals, while (c) and (d) are computed from PPG signals. The spectrogram-based representations of ECG and PPG signals derived from the same individual present visual differences in their patterns and should therefore be matched by using specifically designed techniques. As shown in Fig. 3, the spectrograms obtained from cardiac signals present relevant differences that can also be recognized by human observers.

### 3.3. MultiCardioNet

MultiCardioNet consists of a Siamese CNN designed and trained to obtain strong accuracy while using limited computational resources. In contrast to most of the Siamese CNNs in the literature, which are based on well-known pretrained models, MultiCardioNet consists of a specifically designed model that takes two grayscale images as inputs. Another novelty consists of the training algorithm proposed for MultiCardioNet, which can create an accurate knowledge base of Siamese CNNs from unbalanced datasets composed of limited numbers of samples.

MultiCardioNet is composed of two identical CNNs that share the same weights. Every CNN takes a spectrogram-based image  $S$  as input and computes a set of embeddings  $E$ . Considering two spectrogram-based images  $S_A$  and  $S_B$ , MultiCardioNet computes a matching score  $m_{A,B}$  as the Euclidean distance  $\|E_A - E_B\|$ . Fig. 4 shows the schema of MultiCardioNet.

In the following, we refer to the architecture of the two identical CNNs composing MultiCardioNet as Convnet.

Convnet is a specifically designed CNN that is composed as follows.

1. The input layer accepts grayscale images with sizes of  $28 \times 28$  pixels.
2. Convolutional layer 1 is composed of 16 convolutional filters with sizes of  $5 \times 5$  pixels and rectified linear units (ReLU).
3. A max pooling layer with  $2 \times 2$ -pixel steps is included.
4. Convolutional layer 2 is composed of 32 convolutional filters with sizes of  $3 \times 3$  pixels and ReLUs.
5. A max pooling layer with  $2 \times 2$ -pixel steps is included.
6. Convolutional layer 3 is composed of 64 convolutional filters with sizes of  $3 \times 3$  pixels and ReLUs.

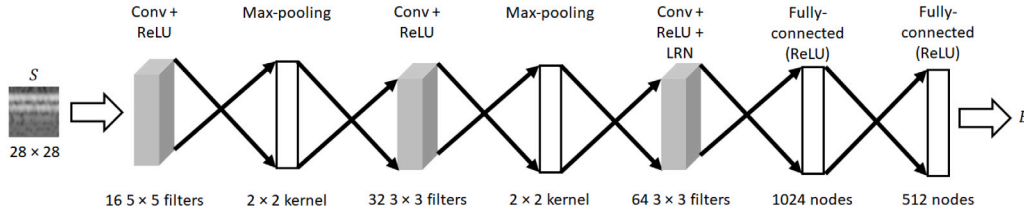


Fig. 5. Schema of Convnet, the CNN used to create MultiCardioNet.

7. Fully connected layer 1 is composed of 1024 ReLU nodes.

8. Fully connected layer 2 is composed of 512 ReLU nodes.

Fig. 5 shows a graphical representation of Convnet.

### 3.4. Training algorithm

To increase the generalization capability of Siamese neural networks for imbalanced datasets composed of relatively small numbers of samples, we propose an ad hoc training algorithm that computes a training set of spectrogram-based image pairs  $P$  every  $n_e$  epochs. The algorithm is applied only to the training partition of the initial dataset, without considering the samples of the testing partition.

Considering  $i$  as the index representing an individual and  $j$  as the number of samples acquired from individual  $i$ , for every sample  $S_{i,j}$ , our training algorithm considers the set of pairs  $P$  as being composed of three subsets  $P = [P_1, P_2, P_3]$ .

- $P_1$  includes every genuine comparison for  $S_{i,j}$ . Specifically,  $P_1$  includes every pair  $[S_{i,j}, S_{i,k}]$ ,  $\forall j \neq k$ . Since this training algorithm aims to cope with biometric datasets composed of small numbers of samples, we design the subset  $P_1$  to train Siamese neural networks with every possible genuine identity comparison.
- $P_2$  includes the  $n_2$  worst impostor comparisons for  $S_{i,j}$ . Specifically, we compute the vector  $C_{i,j}$  representing the normalized cross-correlation between every pair of impostor samples  $[S_{i,j}, S_{l,k}]$ ,  $\forall i \neq l$ .  $S_{i,j}$  is then sorted in descending order according to the values of  $C_{i,j}$ , and the first  $n_2$  pairs of samples are included in  $P_2$ . We design the subset  $P_2$  to increase the interclass distances in the feature space for the worst impostor comparisons. In this case, we select the worst impostor pairs by using the normalized cross-correlation function, which can be substituted by other functions for different application contexts.
- $P_3$  includes  $n_3$  randomly selected impostor pairs that are not included in  $P_2$ . Specifically,  $P_3$  includes  $n_3$  randomly selected samples  $(S_{i,j}, S_{l,k})$ ,  $\forall i \neq l, (S_{i,j}, S_{l,k}) \notin P_2$ . We design the subset  $P_3$  to introduce random data every  $n_e$  training epochs, thus increasing the robustness of the identity verification system and reducing the learning speed of the training process.

## 4. Experimental results

In this section, we first present the experimental protocol and the details of the training process. Then, we analyze the accuracy of the proposed method and the results obtained by different configurations of the proposed learning algorithm.

### 4.1. Experimental protocol

We evaluated the performance of our proposed method by using a publicly available dataset, CapnoBase PRRB [17], which is composed of ECG and PPG signals acquired from 42 subjects (29 children and 13 adults). For both ECG and PPG signals, the sampling rate was equal to 300 Hz, and every acquisition corresponded to a period of 8 min. We considered the ECG signals and only the first PPG channel.

Our method takes fixed-length signals of  $t$  seconds as inputs. We used  $t = 20$  since we considered this time duration to be a good tradeoff

between system usability and the amount of information usable for biometric recognition. Therefore, we obtained 1008 ECG samples and 1008 PPG samples by dividing CapnoBase PRRB into nonoverlapping samples of 20 s.

To analyze the identity verification accuracy of the proposed approach, we considered the following metrics: the equal error rate (EER), the false match rate (FMR), the false nonmatch rate (FNMR), and receiver operating characteristic (ROC) curves [45].

The parameters used to enhance cardiac signals were as follows:  $f_b = 0.5$  Hz,  $f_h = 50$  Hz, and  $f_l = 90$  Hz. The parameters used to compute spectrogram-based images were empirically set to  $m = 600$ ,  $o_m = 400$ , and  $y_c = 56$ .

### 4.2. Training of MultiCardioNet

To train MultiCardioNet, we labeled every pair of genuine comparisons as 1 and every pair of impostor comparisons as 0.

We trained MultiCardioNet separately to compare pairs of different types of signals: ECG-ECG, PPG-PPG, and ECG-PPG/PPG-ECG signals.

We implemented MultiCardioNet in Python by using the TensorFlow library. The weights of the Siamese CNN were trained from scratch by using He uniform initialization for the convolutional and fully connected layers. For the single-domain identity comparisons (ECG-ECG and PPG-PPG), MultiCardioNet was tuned for 100 epochs by using  $n_e = 10$ ,  $n_2 = 23$ , and  $n_3 = 46$ . In this way, almost 1/4 of the sample pairs  $P$  represented genuine comparisons since the considered dataset was composed of 24 comparisons per individual. For multiple-domain identity comparisons (ECG-PPG/PPG-ECG), MultiCardioNet was tuned for 100 epochs by using  $n_e = 10$ ,  $n_2 = 0$ , and  $n_3 = 69$ . Since no direct correspondence was computable by the normalized cross-correlation between the spectrogram-based representations of ECG and PPG signals, all the impostor pairs of  $P$  were randomly selected. We used root mean square propagation (RMSProp) with a batch size equal to 256 and a learning rate equal to 0.001.

### 4.3. Identity verification accuracy

We validated the proposed method by using a 10-fold cross-validation strategy. The obtained results referred to 23,184 genuine comparisons and to 991,872 impostor comparisons. Table 1 summarizes the identity verification accuracy achieved with different configurations of our proposed method, and Fig. 6 shows the obtained ROC curves.

The ECG-ECG scenario yielded an EER of 2.15%. To the best of our knowledge, no results have been reported in the literature for biometric recognition methods using the ECG channel of the used dataset. As a reference, we computed the performance of the correlation-based method presented in [33] for the same dataset by using the same time partitioning strategy, which produced an EER of 4.91%. Although methods based on two-dimensional representations of ECG signals have been tested on different datasets [28–30], the obtained results are comparable with those of the state-of-the-art approaches.

The PPG-PPG scenario yielded an EER of 2.42%. This result was significantly better than that of the only biometric system in the literature for computing two-dimensional representations of PPG signals [15], which obtained an FMR of 0.56% at an FNMR of 13.50% for the same

**Table 1**  
Identity verification accuracy achieved by MultiCardioNet (10-fold cross-validation).

Signal pairs	EER (%)	FMR @ FNMR = 1% (%)
ECG-ECG	2.15	3.97
PPG-PPG	2.42	4.76
ECG-PPG/PPG-ECG	4.89	9.25

dataset (using a slightly different k-fold cross-validation protocol). As a further reference, we computed the performance of the correlation-based method presented in [33] for the same dataset using the same time partitioning strategy, which produced an EER of 14.7%. To the best of our knowledge, the best result reported in the literature for single-channel identity verification consisted of an EER of 1% [31]. It should be considered that the method proposed in [31] uses fiducial points, a different time division of the signals, a quality assessment algorithm, a data augmentation technique, and a more complex preprocessing strategy than that adopted in this work. The obtained results prove that the proposed approach can achieve better or comparable accuracy with respect to the best-performing state-of-the-art methods for the considered dataset of PPG signals.

The ECG-PPG/PPG-ECG scenario, which was addressed for the first time in the literature, yielded an EER of 4.76%. This result can be considered satisfactory since the obtained accuracy was only slightly lower than that achieved in the single-domain scenarios.

#### 4.4. Proposed training algorithm

We evaluated the identity verification accuracy of MultiCardioNet under different configurations of the proposed training algorithm, as described in Section 3.4.

- Conf\_A, with parameters  $n_e = 10$ ,  $n_2 = 23$ , and  $n_3 = 46$ . The algorithm computes the pairs of samples  $P$  every  $n_e$  training epochs by choosing the  $n_2$  worst impostor pairs and randomly selecting  $n_3$  impostor pairs.
- Conf\_B, with parameters  $n_e = 0$ ,  $n_2 = 23$ , and  $n_3 = 46$ . The algorithm computes the pairs of samples  $P$  only one time (before starting the training process).
- Conf\_C, with parameters  $n_e = 10$ ,  $n_2 = 0$ , and  $n_3 = 69$ . The algorithm computes the pairs of samples  $P$  every  $n_e$  training epochs.

When the application requires functioning in one of the three described configurations, it is sufficient to load or enable the corresponding trained network and its related prefiltering strategy, without any subsequent retraining steps.

Table 2 reports the EER obtained for each configuration in every considered application scenario. The results refer to a validation performed by using 90% of the samples for training and 10% of the samples for testing.

Table 2 shows that the best configuration for single-domain identity comparisons (ECG-ECG and PPG-PPG) is Conf\_A. In this case, the selection of the worst impostor pairs based on the normalized cross-correlation between samples increased the interclass distances in the feature space. For multiple-domain identity comparisons (ECG-PPG/PPG-ECG), Conf\_C obtained the best accuracy since the normalized cross-correlation between the spectrogram-based representations of ECG and PPG signals was less effective than it was in the single-domain identity comparisons. In every case, the iterative computation of the training pairs improved the achieved identity recognition accuracy.

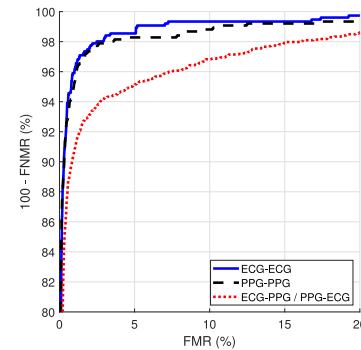


**Fig. 6.** ROC curves obtained for single-domain (ECG-ECG and PPG-PPG) and multiple-domain (ECG-PPG/PPG-ECG) identity verifications.

**Table 2**  
EER (%) values achieved by MultiCardioNet with different configurations of the proposed training algorithm.

Signal pairs	Conf_A	Conf_B	Conf_C
ECG-ECG	1.97	3.57	2.68
PPG-PPG	2.99	4.60	4.60
ECG-PPG/PPG-ECG	4.61	3.37	3.11

## 5. Conclusion

In this paper, we presented a study of the interoperability between ECG and PPG biometrics, marking, to the best of our knowledge, the first exploration of this subject. Our method performs identity verifications by using the proposed MultiCardioNet, a Siamese CNN specifically designed for comparing spectrogram-based representations of cardiac signals and trained with an ad hoc algorithm that we designed to deal with imbalanced datasets composed of limited numbers of samples.

We validated our method on a dataset containing 1,008 pairs of ECG and PPG samples by using a k-fold cross-validation strategy. The results showed that the proposed method could achieve an identity verification accuracy comparable to that of the best-performing techniques in the literature for single-domain configurations. Specifically, the method obtained an EER of 2.15% for ECG-ECG comparisons and an EER of 2.42% for PPG-PPG comparisons. The performance achieved in the multiple-domain configuration (ECG-PPG/PPG-ECG) was also satisfactory since the accuracy reduction with respect to that achieved in the single-domain cases was limited. For the multiple-domain configuration, the proposed method obtained an EER equal to 4.76%. We also analyzed the performance of the proposed training algorithm with different configurations, obtaining the best strategy for single-domain and multiple-domain identity comparisons.

Future work should consider more challenging datasets consisting of signals collected in less-constrained scenarios and for longer time intervals. Furthermore, the proposed method should be integrated into edge devices for monitoring health and sport activities, such as for computing the variability of heart rates derived from both ECG and PPG signals.

### Declaration of competing interest

The authors declare that they have no known competing financial interests or personal relationships that could have appeared to influence the work reported in this paper.

### Data availability

The authors do not have permission to share data

## Acknowledgments

This work was supported in part by the project SERICS (PE00000014) under the NRRP MUR program funded by the EU - NGEU. This work was also supported in part under Edge AI Technologies for Optimised Performance Embedded Processing project, which has received funding from Key Digital Technologies Joint Undertaking (KDT JU) under grant agreement No 101097300. The KDT JU receives support from the European Union's Horizon Europe research and innovation program and Austria, Belgium, France, Greece, Italy, Latvia, Luxembourg, Netherlands, Norway.

## References

- [1] S. Marcel, J.D. R. Millan, Person authentication using brainwaves (EEG) and maximum a posteriori model adaptation, *IEEE Trans. Pattern Anal. Mach. Intell.* 29 (4) (2007) 743–752.
- [2] A. Panzino, G. Orrù, G.L. Marcialis, F. Roli, EEG personal recognition based on 'qualified majority' over signal patches, *IET Biom.* 11 (1) (2022) 63–78.
- [3] A.S. Rathore, Z. Li, W. Zhu, Z. Jin, W. Xu, A survey on heart biometrics, *ACM Comput. Surv.* 53 (6) (2020).
- [4] A. Rattani, W.J. Scheirer, A. Ross, Open set fingerprint spoof detection across novel fabrication materials, *IEEE Trans. Inf. Forensics Secur.* 10 (11) (2015) 2447–2460.
- [5] G. Lavrentyeva, O. Kudashev, A. Melnikov, M. De Marsico, Y. Matveev, Interactive photo liveness for presentation attacks detection, in: *Image Analysis and Recognition*, Springer International Publishing, Cham, 2018, pp. 252–258.
- [6] R. Donida Labati, V. Piuri, R. Sassi, F. Scotti, G. Sforza, Adaptive ECG biometric recognition: a study on re-enrollment methods for QRS signals, in: *Proc. of the IEEE Symposium on Computational Intelligence in Biometrics and Identity Management*, 2014, pp. 30–37.
- [7] T.M.C. Pereira, R.C. Conceição, V. Sencadas, R. Sebastião, Biometric recognition: A systematic review on electrocardiogram data acquisition methods, *Sensors* 23 (3) (2023).
- [8] D. Castaneda, A. Esparza, M. Ghamari, C. Soltanpur, H. Nazeran, A review on wearable photoplethysmography sensors and their potential future applications in health care, *Int. J. Biosens. Bioelectron.* 4 (2018) 195–202.
- [9] A.N. Uwaechia, D.A. Ramli, A comprehensive survey on ECG signals as new biometric modality for human authentication: Recent advances and future challenges, *IEEE Access* 9 (2021) 97760–97802.
- [10] R. Donida Labati, V. Piuri, F. Rundo, F. Scotti, Photoplethysmographic biometrics: A comprehensive survey, *Pattern Recognit. Lett.* 156 (2022) 119–125.
- [11] R. Donida Labati, E. Muñoz, V. Piuri, R. Sassi, F. Scotti, Deep-ECG: Convolutional neural networks for ECG biometric recognition, *Pattern Recognit. Lett.* 126 (2019) 78–85.
- [12] M.S. Islam, H. Alhichri, Y. Bazi, N. Ammour, N. Alajlan, R.M. Jomaa, Heartprint: A dataset of multiresolution ECG signal with long interval captured from fingers for biometric recognition, *Data* 7 (10) (2022).
- [13] D. Biswas, L. Everson, M. Liu, M. Panwar, B. Verhoef, S. Patki, C.H. Kim, A. Acharyya, C. Van Hoof, M. Konijnenburg, N. Van Helleputte, CorNET: Deep learning framework for PPG-based heart rate estimation and biometric identification in ambulant environment, *IEEE Trans. Biomed. Circuits Syst.* 13 (2) (2019) 282–291.
- [14] D. Chicco, Siamese neural networks: An overview, in: H. Cartwright (Ed.), *Artificial Neural Networks*, Springer US, New York, NY, 2021, pp. 73–94.
- [15] R. Donida Labati, V. Piuri, F. Rundo, F. Scotti, C. Spampinato, Biometric recognition of PPG cardiac signals using transformed spectrogram images, in: *Pattern Recognition. ICPR Int. Workshops and Challenges*, Springer Int. Publishing, Cham, 2021, pp. 244–257.
- [16] P. Samarati, S. De Capitani di Vimercati, Cloud security: Issues and concerns, in: S. Murugesan, I. Bojanova (Eds.), *Encyclopedia on Cloud Computing*, Wiley, 2016.
- [17] W. Karlen, M. Turner, E. Cooke, G. Dumont, J.M. Ansermino, CapnoBase: Signal database and tools to collect, share and annotate respiratory signals, in: *Annual Meeting of the Society for Technology in Anesthesia*, West Palm Beach, 2010.
- [18] Z. Zhang, Z. Pi, B. Liu, TROIKA: A general framework for heart rate monitoring using wrist-type photoplethysmographic signals during intensive physical exercise, *IEEE Trans. Biomed. Eng.* 62 (2) (2015) 522–531.
- [19] M. Merone, P. Soda, M. Sansone, C. Sansone, ECG databases for biometric systems: A systematic review, *Expert Syst. Appl.* 67 (2017) 189–202.
- [20] M. Tantawi, A. Salem, M.F. Tolba, Fiducial based approach to ECG biometrics using limited fiducial points, in: A.E. Hassanien, M.F. Tolba, A. Taher Azar (Eds.), *Advanced Machine Learning Technologies and Applications*, Springer International Publishing, Cham, 2014, pp. 199–210.
- [21] Y. Wang, F. Agrafioti, D. Hatzinakos, K.N. Plataniotis, Analysis of human electrocardiogram for biometric recognition, *EURASIP J. Adv. Signal Process.* 2008 (1) (2008) 148658.
- [22] K.N. Plataniotis, D. Hatzinakos, J.K.M. Lee, ECG biometric recognition without fiducial detection, in: *2006 Biometrics Symposium: Special Session on Research At the Biometric Consortium Conf.*, 2006, pp. 1–6.
- [23] P. Melzi, R. Tolosana, R. Vera-Rodriguez, ECG biometric recognition: Review, system proposal, and benchmark evaluation, *IEEE Access* 11 (2023) 15555–15566.
- [24] V. Randazzo, G. Cirrincione, E. Pasero, Shallow neural network for biometrics from the ECG-WATCH, in: D.-S. Huang, V. Bevilacqua, A. Hussain (Eds.), *Intelligent Computing Theories and Application*, Springer International Publishing, Cham, 2020, pp. 259–269.
- [25] H. Kim, T.Q. Phan, W. Hong, S.Y. Chun, Physiology-based augmented deep neural network frameworks for ECG biometrics with short ECG pulses considering varying heart rates, *Pattern Recognit. Lett.* 156 (2022) 1–6.
- [26] D.Y. Hwang, B. Taha, D.S. Lee, D. Hatzinakos, Evaluation of the time stability and uniqueness in PPG-based biometric system, *IEEE Trans. Inf. Forensics Secur.* 16 (2021) 116–130.
- [27] V. Jindal, J. Birjandtalab, M.B. Pouyan, M. Nourani, An adaptive deep learning approach for PPG-based identification, in: *Proc. of the 38th Annual Int. Conf. of the IEEE Engineering in Medicine and Biology Society*, 2016, pp. 6401–6404.
- [28] Y.-H. Byeon, K.-C. Kwak, Pre-configured deep convolutional neural networks with various time-frequency representations for biometrics from ECG signals, *Appl. Sci.* 9 (22) (2019).
- [29] Y. Byeon, S. Pan, K. Kwak, Ensemble deep learning models for ECG-based biometrics, in: *Proc. of the Cybernetics Informatics*, 2020, pp. 1–5.
- [30] I.B. Ciocoiu, N. Cleju, Off-person ECG biometrics using spatial representations and convolutional neural networks, *IEEE Access* 8 (2020) 218966–218981.
- [31] D.Y. Hwang, B. Taha, D.S. Lee, D. Hatzinakos, Evaluation of the time stability and uniqueness in PPG-based biometric system, *IEEE Trans. Inf. Forensics Secur.* 16 (2021) 116–130.
- [32] N. Karimian, Z. Guo, M. Tehranipoor, D. Forte, Human recognition from photoplethysmography (PPG) based on non-fiducial features, in: *Proc. of the IEEE Int. Conf. on Acoustics, Speech and Signal Processing*, 2017, pp. 4636–4640.
- [33] A. Bonissi, R. Donida Labati, L. Perico, R. Sassi, F. Scotti, L. Sparagino, A preliminary study on continuous authentication methods for photoplethysmographic biometrics, in: *Proc. of the IEEE Workshop on Biometric Measurements and Systems for Security and Medical Applications*, 2013, pp. 28–33.
- [34] S.P.M. Namini, S. Rashidi, Implementation of artificial features in improvement of biometrics based PPG, in: *Proc. of the 6th Int. Conf. on Computer and Knowledge Engineering*, 2016, pp. 342–346.
- [35] E. Lee, A. Ho, Y. Wang, C. Huang, C. Lee, Cross-domain adaptation for biometric identification using photoplethysmogram, in: *Proc. of the IEEE Int. Conf. on Acoustics, Speech and Signal Processing*, 2020, pp. 1289–1293.
- [36] D.Y. Hwang, B. Taha, D. Hatzinakos, PBGAN: Learning PPG representations from GAN for time-stable and unique verification system, *Trans. Inf. Forensics Secur.* 16 (2021) 5124–5137.
- [37] S.Z. Fatemian, F. Agrafioti, D. Hatzinakos, Heartid: Cardiac biometric recognition, in: *2010 Fourth IEEE International Conf. on Biometrics: Theory, Applications and Systems*, 2010, pp. 1–5.
- [38] C. Song, S. Ji, Face recognition method based on siamese networks under non-restricted conditions, *IEEE Access* 10 (2022) 40432–40444.
- [39] J. Solano, E. Rivera, L. Tengana, C. López, J. Flórez, M. Ochoa, A siamese neural network for scalable behavioral biometrics authentication, in: *Applied Cryptography and Network Security Workshops*, Springer International Publishing, Cham, 2022, pp. 515–535.
- [40] L. Ivanciu, I.-A. Ivanciu, P. Faragó, M. Roman, S. Hintea, An ECG-based authentication system using siamese neural networks, *J. Med. Biol. Eng.* 41 (2021) 558–570.
- [41] Y. Zhao, J. Li, C. Liu, ECG identification fusion model based on siamese neural networks, in: *Proc. of the 6th International Conf. on Biological Information and Biomedical Engineering*, 2022, pp. 1–6.
- [42] C. Lin, A. Kumar, Multi-siamese networks to accurately match contactless to contact-based fingerprint images, in: *Proc. of the IEEE International Joint Conf. on Biometrics*, 2017, pp. 277–285.
- [43] R. Miller, N.K. Banerjee, S. Banerjee, Using siamese neural networks to perform cross-system behavioral authentication in virtual reality, in: *Proc. of the IEEE Virtual Reality and 3D User Interfaces*, 2021, pp. 140–149.
- [44] F. Schroff, D. Kalenichenko, J. Philbin, FaceNet: A unified embedding for face recognition and clustering, in: *Proc. of the IEEE Conf. on Computer Vision and Pattern Recognition*, 2015.
- [45] A.K. Jain, P. Flynn, A.A. Ross, *Handbook of Biometrics*, first ed., Springer Publishing Company, Incorporated, 2010.